Reactive and Functional Polymers 214 (2025) 106341

Contents lists available at ScienceDirect

Reactive and Functional Polymers

journal homepage: www.elsevier.com/locate/react

Catalytic effect of rare-earth triflates in the relaxation and creep behavior of poly(epoxy imine) vitrimers

Tommaso Telatin [a], Silvia De la Flor [b], Àngels Serra [a,*], Xavier Montané [a,*]

[a] Universitat Rovira i Virgili, Department of Analytical and Organic Chemistry, C/ Marcel·lí Domingo 1, 43007 Tarragona, Spain
[b] Universitat Rovira i Virgili, Department of Mechanical Engineering, Av. Països Catalans 26, 43007 Tarragona, Spain

ARTICLE INFO

Keywords:
Epoxy
Vitrimers
Polyimine
Creep
Amines

ABSTRACT

The catalytic activity of scandium triflate, known for its efficiency in transimination reactions, as well as lanthanum and ytterbium triflates, was explored in promoting imine metathesis reactions in Covalent Adaptable Networks (CANs). In the present work, we focused on a previously examined system where bisphenol A diglycidyl ether (DGEBA) was cured with a telechelic primary amine-terminated polyimine oligomer. The resulting material exhibited vitrimeric behavior ascribable to the imine metathesis reaction. The structure of the oligomer was characterized by ^{1}H NMR and its molecular weight was determined by end-groups analysis, after derivatization with *tert*-butyl isocyanate. To overcome the limitations in the stress relaxation process, caused by the network structure, we explored the addition of some rare-earth triflates to see if they could accelerate the exchange process. Fourier-transform infrared (FTIR) spectroscopy confirmed the absence of by-product formation during the curing process with these catalysts, while differential scanning calorimetry (DSC) was used to assess their potential effects on curing kinetics.

Thermomechanical properties were evaluated through dynamic thermomechanical analysis (DMTA). Our findings revealed a complex effect of the triflate salts on the creep resistance of the materials. These catalysts enhanced deformation stability through imine-metal coordination but simultaneously reduced activation energies for the exchange process, balancing structural integrity with dynamic adaptability.

1. Introduction

Vitrimers are being considered as a sustainable option for recycling thermosetting materials. They consist of a three-dimensional network with exchangeable groups, allowing them to be reshaped or recycled once they reach the end of their service life. Among all the dynamic chemistries suitable for developing vitrimeric materials, the imine metathesis reaction has attracted the interest of many academic researchers for a long time. Zhang et al. [1] designed a catalyst-free malleable polyimine network from commercially available aldehydes and amines, which could be reprocessed by applying water or heat to obtain efficiently recycled samples without the loss of mechanical performance. Subsequently, the same group tested polyimine vitrimers as binders in carbon fiber reinforced composites (CFRC) by adding a single layer carbon fiber fabric, resulting in carbon fiber reinforced composites (CFRCs) that could be easily molded into shapes with three-dimensional (3D) curvatures [2]. Abu-Omar and co-workers were the first to synthesize a diepoxy compound containing an imine group in its structure by condensation of vanillin with 4-aminophenol and subsequent epoxidation reaction of the obtained diphenol product with epichlorohydrin [3]. As a result, they obtained a thermoset material with high mechanical performance and good vitrimeric behavior with short relaxation times even at low temperatures, and demonstrated the high malleability and the self-welding properties of these imine-containing polymers.

Our group made a step forward by developing a fully bio-based epoxy monomer containing imine and disulfide groups, which exhibited extremely fast stress relaxation when cured with different commercial amines [4]. These materials not only resulted fully chemically degradable and mechanically recyclable but also allowed the preparation of CFRCs with competitive mechanical properties.

An alternative route involves the preparation of telechelic linear polyimine oligomers as dynamic hardeners. This route appears to be more suitable for technological applications, as it allows for the use of various types of commercial glycidyl resins. Following this methodology, Liu et al. prepared a series of epoxy vitrimers from diglycidylether

---

* Corresponding authors.
E-mail addresses: angels.serra@urv.cat (À. Serra), xavier.montane@urv.cat (X. Montané).

https://doi.org/10.1016/j.reactfunctpolym.2025.106341
Received 25 April 2025; Received in revised form 14 May 2025; Accepted 18 May 2025
Available online 19 May 2025
1381-5148/© 2025 The Authors. Published by Elsevier B.V. This is an open access article under the CC BY-NC-ND license (http://creativecommons.org/licenses/by-nc-nd/4.0/).

of bisphenol F and a polyimine oligomer prepared from terphthalaldehyde and 3-aminobenzylamine [5]. Our group investigated in detail the effect of the length of the polyimine oligomer and the proportion of two different amines (Jeffamines and diethylendiamine) used in its synthesis in an epoxy-amine system [6]. Promising results were obtained by this approach in modulating the glass transition temperature and tuning the activation energy of the exchange reaction.

In the same context, it is well known that the kinetics of an exchange reaction is reflected in macroscopically measurable material properties, such as the relaxation rate of an applied mechanical stress. From this point of view, several factors affect the kinetics of the process, such as the mobility of the network and the distribution of the dynamic groups in the overall polymeric structure. From this perspective, although the typically rapid exchange reaction in the absence of a catalyst is a defining characteristic of imine metathesis-based materials, incorporating chemical species that can accelerate the exchange process offers a promising strategy to address the limitations imposed by the network structure and achieve higher stress relaxation rates.

Considering kinetic aspects, rare-earth triflates are widely employed as Lewis acid catalysts in organic synthesis. The main advantages of these catalysts over other Lewis acids are their commercial availability, their low toxicity [7], their tolerance to air, moisture, and protic solvents [8], and their ease of handling and recycling. Furthermore, rare-earth cations have low electronegativity and strong oxophilicity, and the effect of the triflate anion, which has an electron withdrawing capacity, increases their Lewis acidity [9]. Moreover, the Lewis acidity and the coordination ability can be modulated by changing the rare-earth metal [10]. Finally, these Lewis acids are very advantageous because they possess a higher activity and less corrosive behavior compared with Brønsted acids [11].

The catalytic activity of triflates of various metals was proved in the reaction between amines and nitriles [12]. In addition, it has been shown that rare-earth triflates are one of the best catalysts for ring-opening polymerization. [13–15] Our group reported their use in the curing of epoxy resins [16,17] and in the copolymerization of epoxy resins with lactones. [18,19] Their use as catalysts in C—C bond-forming reactions has been deeply investigated, demonstrating their versatility in a wide range of organic reactions such as aldol, Michael, allylation, Diels-Alder, Friedel-Crafts, and glycosylation reactions [20]. Moreover, scandium triflate was found to be a promising catalyst in the imine formation [21,22] and in the transimination reaction, [23,24] which is one of the responsible exchange reactions for the stress relaxation in polyimine covalent adaptable networks (CANs). Rare-earth metal triflates have also shown their ability to enhance the relaxation rate of poly (thiourethane) [25] and poly(amido-imide) [26] CANs. Thus, the extreme versatility of these Lewis acids makes them very promising to be used in the field of CANs as catalysts for the exchange reaction.

Taking into account mechanical aspects in vitrimer materials, Schoustra and Smulder explored how metal coordination influences the relaxation and creep resistance of polyimine CANs [27]. Their findings showed that enhancing metal coordination with the imine groups can improve both the material properties and creep resistance. Consequently, adding rare-earth triflates, known for their strong coordination capabilities, to the curing formulation can influence not only the kinetics of stress relaxation but also the curing process and the final properties of the resulting vitrimers. However, it must be noticed that they started from isophthalic aldehyde and 2,6-pyridinedicarboxaldehyde, with proper geometry for excellent coordination.

The present work investigates the catalytic activity of lanthanum, ytterbium and scandium triflates in the preparation of polyimine-based covalent adaptable networks. A previously well-characterized polyimine-epoxy-amine system was employed as a reference system to evaluate these rear earth triflate catalysts [6]. Among all the different materials studied, the one exhibiting the slower stress relaxation behavior was chosen to verify the influence of the Lewis acids on the imine metathesis reaction, which is responsible for the dynamic properties of the system.

A polyimine oligomer was synthesized from commercially available monomers such as terephthalaldehyde (TA), diethylenetriamine (DETA) and the polyetheramine Jeffamine D-230. The molecular weight of the oligomer was calculated by a new implemented methodology consisting in derivatization with *tert*-butyl isocyanate and further evaluation of end groups by ^{1}H NMR spectroscopy. The obtained telechelic amine-terminated polyimine oligomer was cured with a stoichiometric amount of a commercial epoxy resin: bisphenol A diglycidyl ether (DGEBA).

Differential scanning calorimetry (DSC) was used to assess if the catalysts affected the nucleophilic addition of the amines to the oxirane rings during the curing process. The thermal and thermo-mechanical properties were evaluated using thermogravimetric analysis (TGA) and dynamic thermo-mechanical analysis (DMTA), respectively.

Finally, DMTA experiments were conducted to investigate the impact of rare-earth triflates on the creep behavior and vitrimeric properties of the prepared materials.

2. Experimental part

2.1. Materials

The following chemicals were purchased from Sigma-Aldrich: diethylenetriamine (DETA, 99 %), poly(propylene glycol) bis(2-aminopropyl ether) (Jeffamine D-230, M_n ~ 230 g/mol), terephthalaldehyde (TA, 99 %), scandium (III) trifluoromethanesulfonate ($Sc(OTf)_3$, 99 %), lanthanum (III) trifluoromethanesulfonate ($La(OTf)_3$, 99.999 %), ytterbium(III) trifluoromethanesulfonate ($Yb(OTf)_3$, 99.99 %) and *tert*-butyl isocyanate (97 %). Bisphenol A diglycidyl ether (DGEBA, trade name ARALDITE GY240, 5.51 eq/kg) was purchased from Huntsman. 2-Propanol (*i*-PrOH) was purchased from Carlo Erba, and tetrahydrofuran (THF) from Scharlau. All chemicals were used as received.

2.2. Procedure for the synthesis of the polyimine oligomer (D230 50/50 40 %)

The procedure for the synthesis of the polyimine oligomer D230 50/50 40 % was synthetized following a procedure reported by us[6]: In a round bottom flask equipped with a magnetic stirrer and reflux condenser, 1.14 g (8.50 mmol) of TA, 0.61 g (5.95 mmol) of DETA and 1.37 g (5.95 mmol) of Jeffamine D-230 were dissolved in 50 mL of a mixture of THF and *i*-PrOH (3/1 *v*/v). The reaction mixture was magnetically stirred and maintained at 60 °C for 2 h. After that, the mixture of solvents was removed under reduced pressure, and the sample was dried under vacuum at 80 °C for 24 h. The name of the oligomer D230 50/50 40 % indicates a 50 % of DETA and a 50 % of Jeffamine in the oligomer preparation and the 40 % indicates the excess of DETA and Jeffamine together in reference to the terphthalaldehyde.

2.3. Characterization of the imine oligomer

The imine oligomer was characterized by ^{1}H and [] ^{13}C NMR spectroscopy. Both spectra are collected in the supporting information (**Figs. S1** and **S2**).

The determination of the average molecular weight was done by analyzing terminal groups after derivatization of the amine telechelic monomer with *tert*-butyl isocyanate. With this reaction, primary amines, at the end groups, and secondary amines, from the DETA unit, were converted into the corresponding urethane groups. The molecular weight of the oligomer was determined by ^{1}H NMR spectroscopy by comparing the integrations of the end group signals with the integrations of aromatic protons in the derivatized oligomer as reported in the Supporting Information.

2.4. Procedure for the preparation of vitrimeric samples

The polyimine-epoxy vitrimers were obtained according to the following procedure: 3.12 g of polyimine oligomer were mixed with 3.55 g of DGEBA and dissolved in THF. We added to the previous mixture a 1 % in mol of the selected catalyst with respect to the mol of imine groups and the mixture was stirred until complete dissolution. Finally, the solvent was evaporated under vacuum at 40 °C and poured into a rectangular Teflon mold of 30 × 5 × 1.5 mm^3. The samples were cured in an oven using the following schedule: 3 h at 100 °C, 2 h at 150 °C, and 2 h at 180 °C.

2.5. Characterization techniques

A Jasco FT/IR-680 Plus spectrometer, fitted with an attenuated total reflection (ATR) accessory (Golden Gate, Specac Ltd., Teknokroma), was utilized to obtain the Fourier transform infrared (FTIR) spectra of the prepared materials after the curing process. Real-time spectra were recorded over a wavenumber range of 4000 to 600 cm^{-1} with a resolution of 4 cm^{-1}, averaging 20 scans. The completion of the reaction was confirmed by the disappearance of the characteristic epoxy band attributed to the asymmetric ν(-C-O-C-) that appears at 915 cm^{-1} and the emergence of the band attributed to the ν(O—H) at around 3300 cm^{-1}.

The thermal stability of the materials was evaluated using a Mettler Toledo TGA 2 thermobalance. Cured samples weighing around 10 mg were degraded between 30 and 600 °C at a heating rate of 10 °C min^{-1} in N_2 atmosphere with a flow rate of 50 cm^3 min^{-1}.

DSC analyses were carried out on a Mettler DSC3+ instrument calibrated using indium (heat flow calibration) and zinc (temperature calibration) standards. Samples of approximately 8–10 mg were placed in aluminum pans with pierced lids and analyzed in an N_2 atmosphere with a gas flow of 50 cm^3 min^{-1}. Dynamic studies between −5 and 250 °C at a heating rate of 2 °C min^{-1} were performed.

The thermomechanical properties were studied using a DMTA Q850 (TA Instruments) equipped with a film tension clamp. Prismatic rectangular samples with dimensions of around 30 × 5 × 1.5 mm^3 were analyzed from −10 to 180 °C at 1 Hz, with 0.1 % strain at a heating rate of 2 °C min^{-1}. Tensile stress-relaxation tests were conducted in the same instrument using the film tension clamp on samples with the same dimensions as previously defined. The samples were first equilibrated at the relaxation temperature for 5 min, and a constant strain of 1 % was applied, measuring the consequent stress level as a function of time. The materials were tested only once at one temperature. Creep tests were conducted using the same DMTA Q850 instrument. The sample was equilibrated at 30 °C for 5 min, after which a constant stress (σ) was applied for 30 min and then released. The strain (ε) was measured as a function of time during the application of the stress and for an additional 30 min for the stress recovery. The applied stress was chosen ensuring that each material was in its viscoelastic range. The temperature of 30 °C was chosen as representative of common service conditions.

3. Results and discussion

3.1. Preparation and characterization of the oligomer

The polyimine oligomer was synthesized by condensation reaction of terephthalaldehyde (TA) with diethylenetriamine (DETA) and either Jeffamine D-230 at 60 °C for 2 h in a mixture of THF and 2-propanol (3/1 ν/v) (Scheme 1) following a previously reported procedure [6].

The molecular weight of the oligomer was determined by end-group analysis of the derivatized oligomer. The derivatization was carried out in a $CDCl_3$ solution by adding *tert*-butyl isocyanate in stoichiometric proportion with respect to the number of equivalents of primary and secondary amines of the polyimine oligomer. After 30 min, the ^1H NMR spectrum of the derivatized oligomer was recorded. In the resulting ^1H NMR spectrum, which is shown in Fig. 1, the signal of the methyl protons of the *tert*-butyl groups is observed at 1.32 ppm in the magnified spectral region between 1.30 and 1.38 ppm.

The reaction between the amine groups of the oligomer and the isocyanate led to the instantaneous and quantitative conversion of amines into urea groups. Moreover, the use of isocyanate allowed total selectivity of the target groups without any alteration of the oligomer structure as observable by comparing the spectrum of the derivatized oligomer with the spectrum of the underivatized oligomer (**Fig. S1**).

The signal of the methyl protons of the *tert*-butyl groups is the result of the sum of the signals of the methyl protons from the urea groups obtained from the reaction of the primary amines of the end-groups of the oligomer chains and the urea groups that derived from the reaction of the secondary amines from DETA, located along the oligomeric chains. Taking into account the composition parameter *r*, which describes the proportion of primary amines with respect to aldehyde in the polycondensation reaction, and the proportion between DETA and Jeffamine D-230, the single contribution of the end-groups to the overall signal was calculated following the procedure described in the **Supporting Information**. The obtained integral is representative of the oligomer end-groups and was used to calculate the degree of polymerization (DP) of the oligomer by comparing the relative proton peak

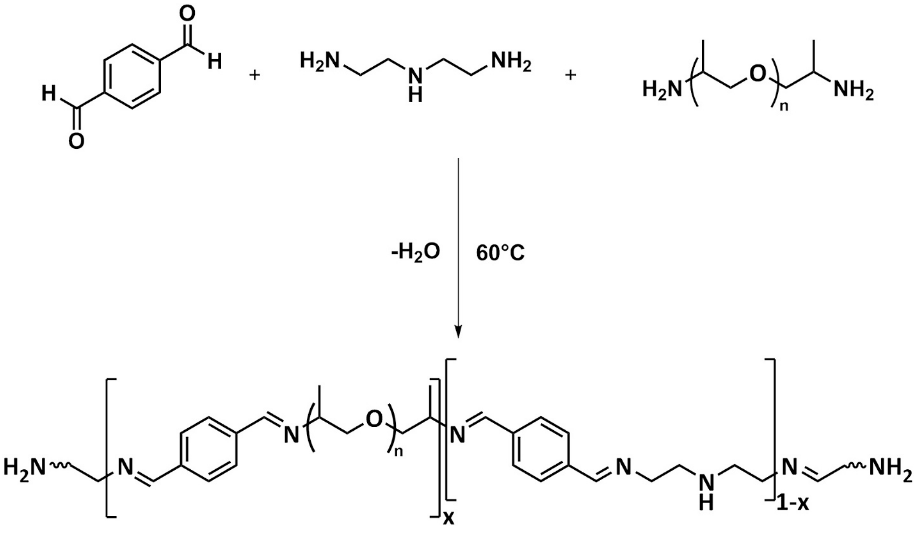

Scheme 1. Scheme of the synthesis of the polyimine oligomer.

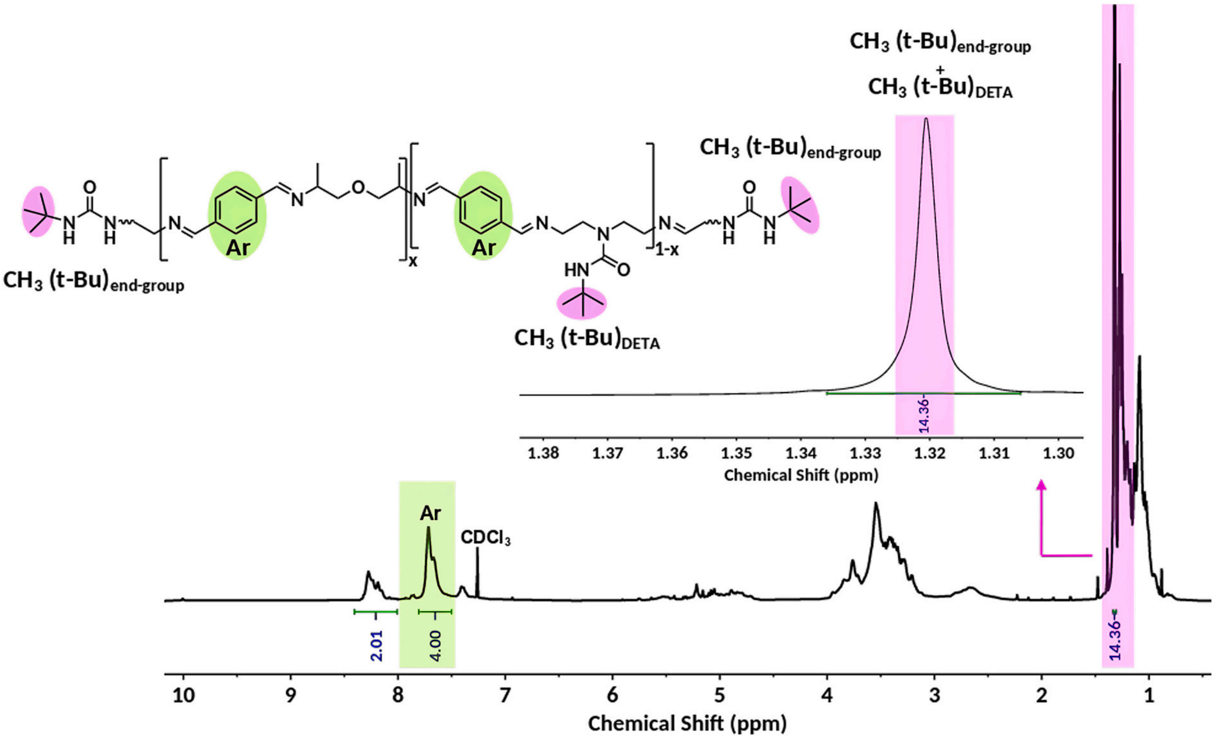

Fig. 1. ^1H NMR spectrum of the *tert*-butyl isocyanate derivative of the polyimine oligomer in $CDCl_3$.

intensity of the end-groups to that of the protons of the aromatic rings, which is representative of the repeating units. According to this information, the number average molecular weight (M_n) of the polyimine-based oligomer was finally calculated ($M_n = 719.63$ g/mol).

3.2. Calorimetric study of the curing procedure

The polyimine oligomer was mixed with DGEBA for each prepared material, ensuring stoichiometric proportion between amine groups (from primary and secondary amines) and epoxy groups. The different catalysts were added at a proportion of 1 % mol of rare-earth triflate catalyst relative to the mol of imine groups, allowing for a comparison of their catalytic activities in the imine metathesis reaction. Larger amounts of catalyst could not be added because the corresponding salt was difficult to solubilize in the reactive mixture.

The curing process is a critical stage in the preparation of cross-linked polymers. In particular, the trigger temperature of the curing reaction strongly affects the workability of the mixture before curing with a great impact on the manufacturing conditions. In light of this, the eventual effects of the rare-earth triflates on the curing process were studied. The use of rare-earth triflates in the aminolysis of epoxides has been reported for some time [28]. As a result, adding these catalysts to the formulation could accelerate the reaction too much, complicating the material processing.

The catalytic activity of the different rare-earth triflates in the nucleophilic addition of the amine terminated oligomer to the oxirane rings of DGEBA was investigated by DSC, and the obtained curves are shown in Fig. 2. The most significant data extracted from DSC tests are collected in Table 1.

All the formulations investigated display an exothermic peak related to the nucleophilic addition of amine groups to the epoxy rings. As illustrated in Fig. 2, adding rare-earth triflates to the curing mixture does not significantly alter the position of this peak. $Yb(OTf)_3$ induces the most significant shift in the temperature of the maximum of the peak, decreasing it from 94 °C to 79 °C. Nonetheless, the temperature variations in the peak maxima are negligible compared to the broadness of the peaks, indicating that the Lewis acids employed do not significantly influence the curing process or the processability of the formulation.

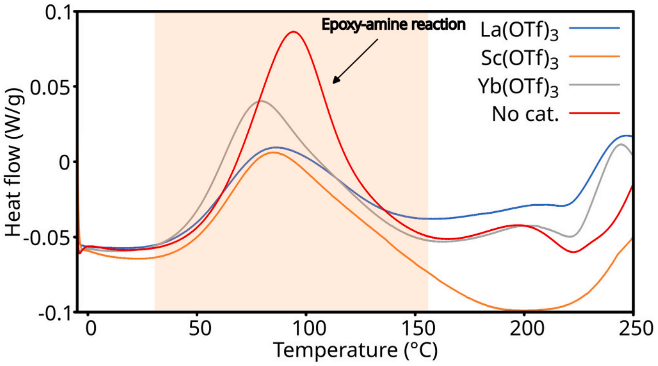

Fig. 2. DSC curves for the curing process of the formulations in presence of the different Lewis acids and without any catalyst.

The structural characterization of the materials was conducted using FTIR analysis. Fig. 3 displays the different spectra, where the complete absence of the epoxy absorption band at 915 cm^{-1}, which is attributed to the asymmetric ν(-C-O-C-), clearly indicates that curing has been fully achieved in all the materials. Moreover, characteristic bands of the cured material are observed in the spectra: the broad ν(O—H) band centered at around 3300 cm^{-1}; the typical imine band at 1663 cm^{-1} ν(C=N); the bands at 1611, 1508 cm^{-1} (attributed to the ν(C=C)), and 829 cm^{-1} (γ(C—H)) corresponding to the aromatic ring. Besides, the bands at 1224, 1091 and 1033 cm^{-1} (attributed to the ν(C-O-C) of the aromatic ethers), together with the band 1182 cm^{-1} (attributed to the ν(C-O-C) of the aliphatic ethers) are also observed. Another important aspect is that there is no variation among the spectra of the different materials prepared, with the only exception of the weak band at around 640 cm^{-1} of the catalyzed materials assigned to the symmetric deformation of the $-SO_3^-$ group of the catalysts [29]. This fact confirms that the rare-earth triflate catalysts enable curing without any side reactions.

Table 1

Calorimetric, thermogravimetric and thermomechanical data for the prepared materials.

Sample	T_{max}[a] (°C)	$T_{1\%}$[b] (°C)	$T_{2\%}$[c] (°C)	T_{max}[d] (°C)	Char yield[e] (%)	$T_{tan\delta}$[f] (°C)	E'_{Glass}[g] (MPa)	$E'_{Rubbery}$[h] (MPa)	Crosslink density[i] (mol/m^3)
No catalyst	94	269	289	366	21	93.6	1681	18	1822
La(OTf)$_3$	85	264	285	385	21	91.5	2117	20	2035
Yb(OTf)$_3$	79	262	285	388	20	91.9	2223	22	2233
Sc(OTf)$_3$	82	254	288	385	20	100.8	2348	28	2779

[a] Temperature of the maximum of the DSC exothermic peak related to the epoxy-amine reaction.

[b] Temperature of 1 % of weight loss.

[c] Temperature of 2 % of weight loss.

[d] Temperature of the maximum rate of degradation.

[e] Char residue at 600 °C.

[f] Temperature at the maximum of tan δ peak at 1 Hz.

[g] Storage modulus in the glassy state (at $T_{tan\ \delta}$ - 50 °C).

[h] Storage modulus in the rubbery state (at $T_{tan\ \delta}$ + 50 °C).

[i] Cross-link density calculated from the storage modulus in the rubbery state.

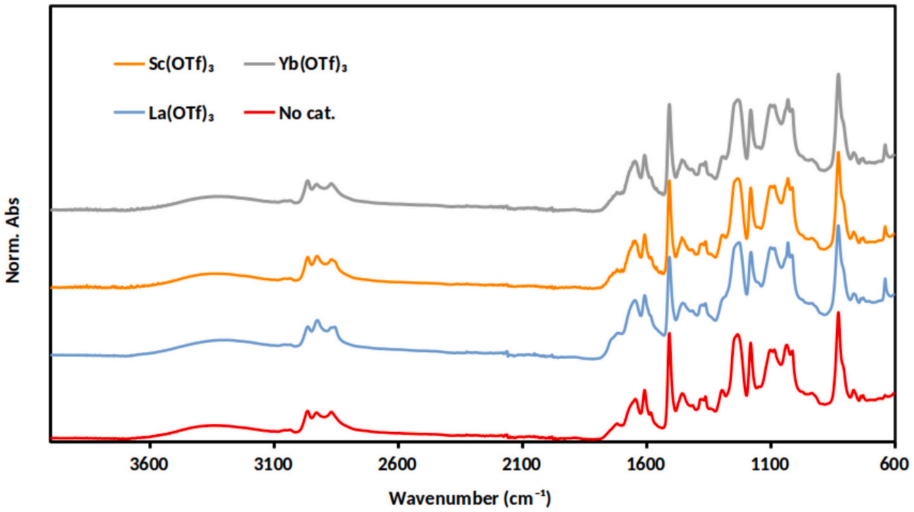

Fig. 3. FTIR spectra of the materials prepared with the following catalysts: Sc(OTf)$_3$, La(OTf)$_3$, and Yb(OTf)$_3$, as well as the material prepared without any catalyst.

3.3. Evaluation of the thermal stability of the materials

The thermal stability of the prepared polyimine cross-linked materials was evaluated by thermogravimetry, and the main data extracted are collected in Table 1. Fig. 4 shows the weight loss plots and their derivatives (DTG curves) for all samples, both the material prepared without any catalyst and those containing 1 % mol rare-earth triflate. The evaluation of the thermal stability of these materials is crucial to prevent degradation during the recycling process.

No significant differences were observed between the materials prepared with rare-earth triflate catalysts and the polymer synthesized without any catalyst, resulting all of them stable up to at least 254 °C, the lowest temperature at which a 1 % of weight loss was detected. The first derivative of the thermogravimetric curves shows a slight shift of the degradation peak to lower temperatures and a slightly higher degradation rate with the addition of a catalyst (Fig. 4b). Furthermore, the char yield was not affected by the presence of the rare-earth triflate catalysts. These results prove that rare-earth triflate catalysts do not compromise the thermal stability of the polyimine-epoxy system. In previous studies from our group, a notable reduction in thermal stability was observed in thermosets produced by copolymerizing DGEBA with lactones when rare-earth triflates were used as catalysts [19]. However, it was shown that the degradation in those cases resulted from a β-elimination process of ester groups, which are absent in the DGEBA-

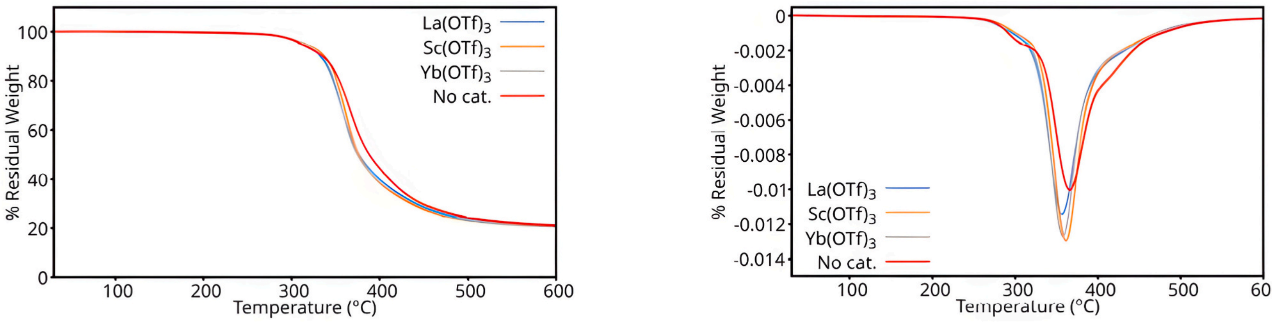

Fig. 4. a) TGA and b) DTG curves of the prepared materials, recorded at 10 °C min^{-1} in N_2 atmosphere.

polyimine materials [30].

3.4. Evaluation of the thermomechanical properties

Thermomechanical properties were determined by DMTA. Fig. 5 shows the storage modulus (E′) and tan δ as a function of temperature for the prepared materials. Moreover, from the storage modulus in the rubbery state the crosslink density was calculated for all the materials using the relationship described by **Equation 1.**[32]

$$d = \frac{E'_{Rubbery}}{3R(Tg - \tan\delta + 40)} 10^6 \tag{1}$$

where d is the crosslink density, E'_{Rubbery} is the storage modulus in the rubbery state (in Pa), R is the gas constant, and $T_{g\text{-}\tan\delta}$ is the temperature of the maximum of the tan δ curve.

The main thermomechanical data obtained from those experiments are collected in Table 1.

Observing the tan δ evolution with temperature for the different materials reveals no significant differences. All materials exhibit a maximum of the tan δ peak around 91 °C, except for the material with $Sc(OTf)_3$ as a catalyst, whose peak maximum appears around 100 °C.

The storage modulus was particularly affected by the presence of rare-earth triflate catalysts in the polymer network. In the glassy state, an increase in E' from 1681 to 2348 MPa was observed using $Sc(OTf)_3$ as a catalyst, while $La(OTf)_3$ and $Yb(OTf)_3$ produced slightly lower increases to 2223 MPa and 2348 MPa, respectively. A similar effect was observed for the storage modulus in the rubbery state, where the scandium salt led again to the most noticeable increase. Considering the atomic properties of the catalysts' metals, a relationship between the storage moduli in the rubbery state and the ionic radius trend is evident. Moreover, for the elements in group 3 of the periodic table, the ability to form complexes strongly depends on the metal ion size [31], suggesting that the metal ions coordinate differently with the imine basic centers present in the network. In this way, a highly crosslinked network is obtained in the presence of a metal triflate catalyst, as any metal center consists of a crosslinking point enhancing material rigidity. Since the storage modulus in the rubbery state is a consequence of the crosslinking density as described by Eq. 1 [32], the observed E' values and consequently the calculated crosslink densities are consistent with this hypothesis. Scandium, the smallest ion and hence the strongest complexing agent among the studied metal catalysts, determined the higher E'. Lanthanum, on the other side, exhibits the bigger ionic radius, and therefore, it affected the cross-linking density of the material in a less pronounced way. Finally, Ytterbium intermediate ion dimensions reflect in the E' in the glassy and in the rubbery states, both included between the E' values of $Sc(OTf)_3$ and $La(OTf)_3$ catalyzed materials. These results are in accordance with what was observed by Schoustra et al., who investigated the effect of a broad series of metal ions on the thermomechanical properties of pure polyimine materials [27].

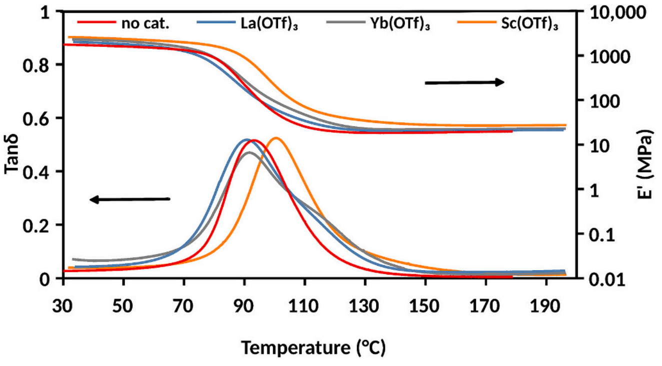

Fig. 5. Evolution of storage modulus and tan δ with temperature for the prepared materials.

3.5. Characterization of the vitrimeric properties

The vitrimeric behavior of the prepared materials was investigated by stress relaxation experiments conducted in tension mode in a range of temperatures between 150 and 200 °C, well above the T_g, to allow the movement of the network structure to perform the exchange process.

The evolution of the normalized stress was monitored as a function of time, and the normalized stress relaxation profiles were fitted to the Kohlrausch-Williams-Watts (KKW) stretched exponential decay function:

$$\frac{E'}{E'_0} = \frac{E'_{perm}}{E'_0} + \left(1 - \frac{E'_{perm}}{E'_0}\right) e^{-\left(\frac{t}{\tau}\right)^{\beta}} \tag{2}$$

where E'/E_0 is the is the normalized stress at relaxation time t, E'_{perm}/E_0 is the fraction of residual stress that remains as the time approaches infinity, τ is a characteristic relaxation time, and β *is* the stretching parameter ($0 < \beta \leq 1$) that described the breadth of the relaxation distribution [33].

Fig. 6 shows the fits by KWW functions superimposed to the stress relaxation modulus profiles for the prepared materials, while Table 2 groups the obtained fitting parameters.

The stretched parameter β was generally high for these materials, ranging between 0.79 and 0.98, demonstrating narrow distributions of the stress relaxation profiles (times).

When rare-earth triflates are used as catalysts a decrease in relaxation times can be generally observed, suggesting that rare-earth triflates have a catalytic effect on the imine metathesis reaction. In agreement with what was discussed in section 3.4, the fractions of residual stress E'_{perm}/E_0 are higher in the presence of the catalysts. Indeed, It can be ascribed to the formation of permanent dative bonds between the metal centers and imines that increase the crosslinking density of the percolated permanent network, generally responsible for the presence of residual stress [33].

The Arrhenius plot, which shows the characteristic relaxation times against the inverse absolute temperature (Fig. 7), and the main data extracted (Table 3) confirm this observation.

Considering the relative acidity of the metal cations ($Sc^{3+} > Yb^{3+} > La^{3+}$) [34], a relationship with the activation energy (E_a) of the exchange process can be identified.

$La(OTf)_3$, the less acidic among the metal triflates selected in this study, produced the highest reduction of the E_a, from 60 kJ/mol for the material without any catalyst to 28 kJ/mol, despite its lower acidity compared to $Sc(OTf)_3$, which conversely determines an increase of E_a, to 78 kJ/mol. Finally, $Yb(OTf)_3$, characterized by intermediate acidic properties, exhibits the lowest catalytic activity, resulting in the same activation energy (61 kJ/mol) of the pristine material.

As observed, while $La(OTf)_3$ led to shorter relaxation times associated with a strongly reduced activation energy, $Sc(OTf)_3$ still reduced the relaxation times but, from the other side, increased the activation energies of the exchange process resulting in faster relaxation at high temperature and almost unaltered relaxation times at low temperature compared to the non catalyzed material. These results suggested that using $Sc(OTf)_3$ could achieve faster stress relaxation at high temperatures, improving material reprocessability without compromising its thermo-mechanical resistance at lower temperatures.

Hence, as reported by Giuseppone and co-workers for the transamination reaction in solvent medium, rare-earth triflates were found to catalyze imine metathesis reaction in the context of a vitrimeric material [23].

3.6. Creep experiments

Creep recovery experiments were performed to evaluate the

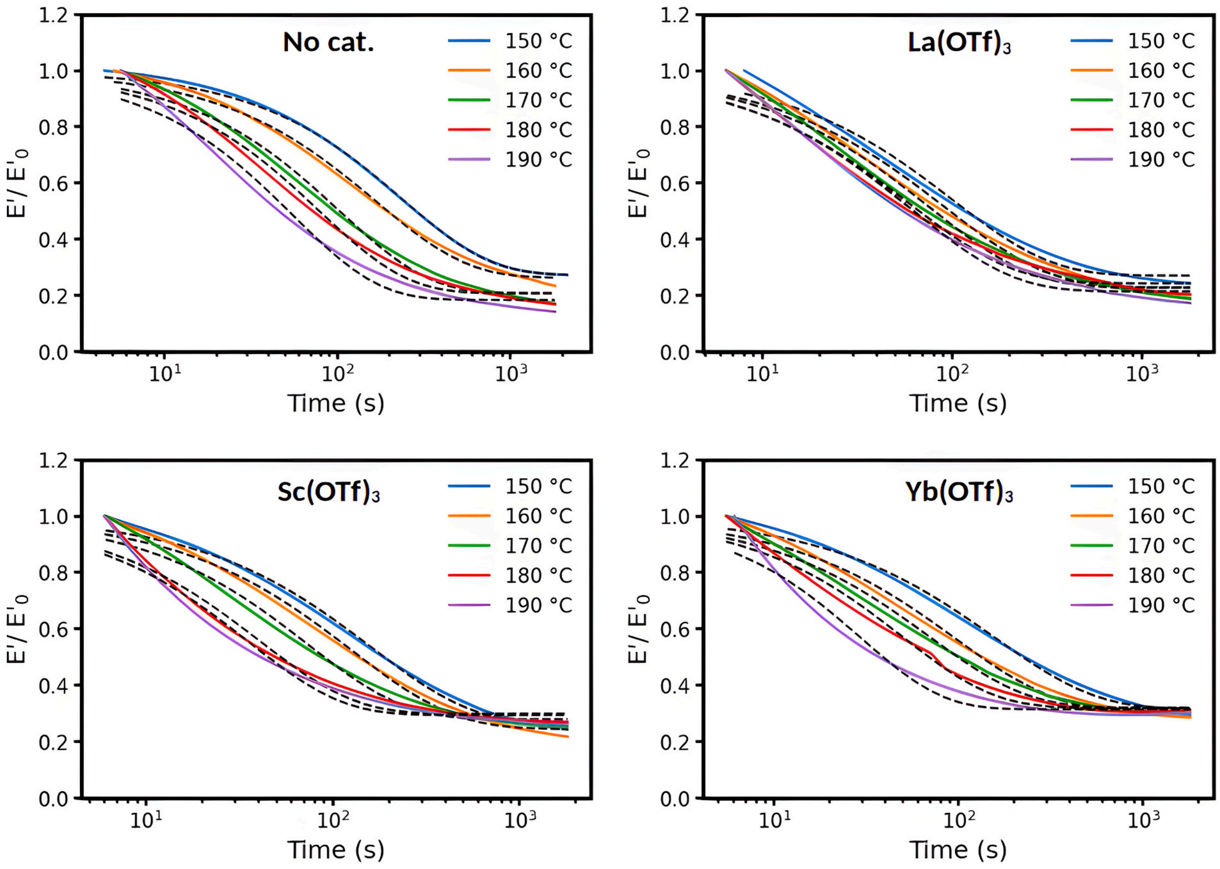

Fig. 6. Normalized curves for the stress relaxation modulus for the prepared materials at different temperatures fitted by a KKW function. The fits are superimposed in black.

Table 2
Fitted parameters for the KKW model at the tested temperature for the prepared materials.

Sample	*T* (°C)	*β*	*τ* (s)	E'_{perm}/E_0	R^2
No catalyst	150	0.86	239	0.27	0.999
	160	0.82	137	0.26	0.995
	170	0.84	103	0.20	0.991
	180	0.86	79	0.20	0.988
	190	0.88	55	0.18	0.982
$La(OTf)_3$	150	0.84	101	0.27	0.987
	160	0.80	92	0.23	0.986
	170	0.82	77	0.23	0.983
	180	0.80	61	0.24	0.987
	190	0.82	52	0.21	0.978
$Yb(OTf)_3$	150	0.80	138	0.32	0.994
	160	0.81	97	0.31	0.990
	170	0.83	70	0.32	0.988
	180	0.89	50	0.32	0.986
	190	0.98	30	0.31	0.969
$Sc(OTf)_3$	150	0.80	161	0.26	0.995
	160	0.79	127	0.24	0.993
	170	0.84	74	0.28	0.986
	180	0.86	41	0.30	0.973
	190	0.87	25	0.29	0.966

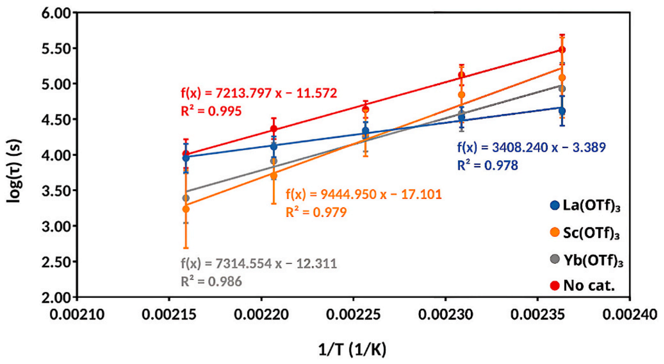

Fig. 7. Arrhenius plot of the stress relaxation behavior of the studied materials.

Table 3
Main data extracted from the Arrhenius plots.

Sample	E_a (kJ/mol)	*lnA*	R^2
No catalyst	60 ± 8	11.6 ± 2.1	0.995
$La(OTf)_3$	28 ± 8	3.4 ± 2.1	0.978
$Yb(OTf)_3$	61 ± 13	12.3 ± 3.7	0.985
$Sc(OTf)_3$	78 ± 21	17.1 ± 5.7	0.979

viscoelastic response of all the vitrimers at 30 °C. The resulting normalized strain *vs.* time curves are shown in Fig. 8.

In agreement with the E_a of the stress relaxation process extracted from the Arrhenius plot in section 3.5., the presence of $La(OTf)_3$ significantly affects the creep resistance of the prepared polyimine-based material. Indeed, it drastically reduces the E_a of the imine metathesis reaction, dropping the temperature at which the exchange reactions start to affect the mechanical properties of the materials. Consequently, the exchange reaction is not negligible at 30 °C and determines a higher creep rate and residual deformation than the non-catalyzed system (Table 4). The main creep parameters at 150 and 190 °C are given in the supporting information as Table S1 and S2, respectively.

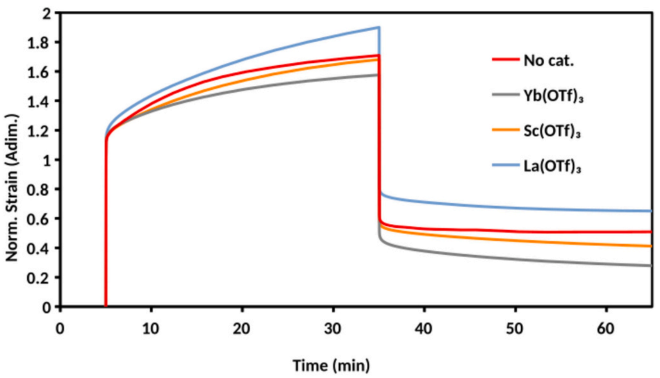

Fig. 8. Creep experiments at 30 °C for all the prepared materials.

Table 4
Main creep parameters at 30 °C for the studied materials.

Sample	$d\varepsilon/dt$ [a]	Residual deformation[b]
No catalyst	$7.5 \cdot 10^{-3}$	0.51
$La(OTf)_3$	$15.3 \cdot 10^{-3}$	0.65
$Yb(OTf)_3$	$6.5 \cdot 10^{-3}$	0.25
$Sc(OTf)_3$	$9.4 \cdot 10^{-3}$	0.38

[a] Determined from the slope of the steady-state region of the creep curve.
[b] Determined after 30 min of releasing the stress.

Conversely, $Sc(OTf)_3$ does not increase the creep rate and the residual deformation of the material at 30 °C, owing to its higher E_a for the exchange process. This higher activation energy results in enhanced exchange rates at elevated temperatures but diminished reactivity at lower temperatures.

The material containing $Yb(OTf)_3$ exhibits the lowest creep rate, and coherently reduced residual deformation compared to the non-catalyzed system, despite having a similar activation energy. This behavior could be attributed to the ability of these triflate salts to coordinate the imine groups within the vitrimeric network. Indeed, Smulders and *co*-workers reported that metal coordination with dynamic covalent imine groups can significantly enhance the mechanical properties and creep resistance of polyimine CANs [27].

Since the E_a of the material containing $Sc(OTf)_3$ is higher than that of the sample prepared with $Yb(OTf)_3$, it would be expected to exhibit variations in the resistance to creep at higher temperatures. However, the observed result is the opposite. Creep experiments at 150 and 190 °C corroborated these results, showing the lower creep susceptibility of $Yb(OTf)_3$ at high temperatures compared to the other catalyzed materials (**Fig. S3** and **Table S1-S2**).

In conclusion, introducing $La(OTf)_3$ led to the highest creep susceptibility, as expected due to the drop in activation energy it produces. In contrast, $Sc(OTf)_3$ and $Yb(OTf)_3$ either increased or maintained the activation energy of the exchange process, thereby reducing the creep deformation and improving the creep recovery.

4. Conclusions

The catalytic effects of rare-earth triflates, specifically $Sc(OTf)_3$, $La(OTf)_3$ and $Yb(OTf)_3$, on the imine metathesis exchange reaction were investigated within an imine-based vitrimeric material. This material was prepared by curing a commercial epoxy resin with an amine-terminated polyimine oligomer.

The derivatization of the synthesized polyimine oligomer with *tert*-butyl isocyanate, followed by characterization using ^1H NMR spectroscopy, proved to be an excellent procedure for determining its molecular weight through end-group analysis.

DSC studies confirmed that the incorporation of these triflate salts into the reactive mixture does not significantly alter the kinetics of the epoxy-amine reaction, demonstrating that the curing process remains practically unaffected. Moreover, FTIR studies demonstrated that adding rare-earth triflates did not modify the chemical structure of the resulting polymer networks.

Stress relaxation experiments revealed a general reduction in relaxation times, but only in the case of $La(OTf)_3$, the catalyst led to a drop in the activation energy. $Sc(OTf)_3$ determined a higher E_a for the exchange process, resulting in a suitable catalyst for preparing imine vitrimers with enhanced processability at high temperatures without compromising the thermo-mechanical performance at low temperatures. Creep experiments corroborated these findings demonstrating the superior creep resistance conferred by $Sc(OTf)_3$ at service temperature. On the other hand, the strong reduction of the activation energy produced by $La(OTf)_3$ for the exchange process facilitates creep, as the material becomes more prone to molecular rearrangements.

Finally, coordination phenomena between the metal cations and the imine groups in the polymer network were found to significantly affect the thermo-mechanical behavior of the studied materials. Generally, higher storage moduli in the glassy and rubbery states were observed for the materials containing the triflate salts. Moreover, metallic coordination of the imine groups improves the network stiffness, as seen for $Yb(OTf)_3$ catalyzed material, which exhibited improved resistance to deformation despite the activation energy was unchanged compared to the non-catalyzed system.

CRediT authorship contribution statement

Tommaso Telatin: Writing – original draft, Methodology, Investigation, Data curation. **Silvia De la Flor:** Writing – review & editing, Supervision, Methodology, Funding acquisition, Data curation. **Àngels Serra:** Writing – review & editing, Supervision, Funding acquisition, Formal analysis, Conceptualization. **Xavier Montané:** Writing – review & editing, Supervision, Formal analysis, Conceptualization.

Declaration of competing interest

The financial suport for this work has been provided by Universitat Rovira i Virgili, Ministerio de Ciencia, Investigación y Universidades and Generalitat de Catalunya Ministry of Research and Universities.

Acknowledgements

This work is part of the R&D projects PID2023-147128OB-C22 and TED2021-131102B-C22, funded by MCIU/AEI/10.13039/501100011033 and European Union Next Generation EU/PRTR. This work was also supported by the Generalitat de Catalunya, grant number 2021-SGR-00154.

Appendix A. Supplementary data

Supplementary data to this article can be found online at https://doi.org/10.1016/j.reactfunctpolym.2025.106341.

Data availability

The raw data required to reproduce these findings cannot be shared at this time due to technical limitations, but supplementary information will be sent on request.

References

[1] P. Taynton, K. Yu, R.K. Shoemaker, Y. Jin, H.J. Qi, W. Zhang, Heat- or water driven malleability in a highly recyclable covalent network polymer, Adv. Mater. 26 (2014) 3938–3942, https://doi.org/10.1002/adma.201400317.
[2] P. Taynton, H. Ni, C. Zhu, K. Yu, S. Loob, Y. Jin, H.Q. Qi, W. Zhang, Repairable woven carbon Fiber composites with full recyclability enabled by malleable

Polyimine networks, Adv. Mater. 28 (2016) 2904–2909, https://doi.org/10.1002/adma.201505245.

[3] S. Zhao, M.M. Abu-Omar, Recyclable and malleable epoxy thermoset bearing aromatic imine bonds, Macromolecules 51 (2018) 9816–9824, https://doi.org/10.1021/acs.macromol.8b01976.

[4] P. Verdugo, D. Santiago, S. De la Flor, A. Serra, A biobased epoxy Vitrimer with dual relaxation mechanism: a promising material for renewable, reusable, and recyclable adhesives and composites, ACS Sustain. Chem. Eng. 12 (2024) 5965–5978, https://doi.org/10.1021/acssuschemeng.4c00205.

[5] H. Liu, H. Zhang, H. Wang, X. Huang, G. Huang, J. Wu, Weldable, malleable and programmable epoxy vitrimers with high mechanical properties and water insensitivity, Chem. Eng. J. 368 (2019) 61–70, https://doi.org/10.1016/j.cej.2019.02.177.

[6] T. Telatin, S. De la Flor, À. Serra, X. Montané, Poly(epoxy-imine) vitrimers., Effect of the structure on the stress relaxation and creep resistance, Polym. Test. 135 (2024) 108465, https://doi.org/10.1016/j.polymertesting.2024.108465.

[7] S. Hirano, K.T. Suzuki, Exposure, metabolism, and toxicity of rare earths and related compounds, Environ. Health Perspect. 104 (1996) 85–95, https://doi.org/10.2307/3432699.

[8] S. Kobayashi, Rare earth metal trifluoromethanesulfonates as water-tolerant Lewis acid catalysts in organic synthesis, Synlett (1994) 689–701, https://doi.org/10.1055/s-1994-22976.

[9] C.G. Fortuna, G. Musumarra, M. Nardi, A. Procopio, G. Sindona, S. Scirè, Principal properties (PPs) for lanthanide triflates as Lewis-acid catalysts, J. Chemom. 20 (2006) 418–424, https://doi.org/10.1002/cem.1016.

[10] C. Huang (Ed.), Rare Earth Coordination Chemistry. Fundamentals and Applications, John Wiley & Sons, Singapore, 2010.

[11] H. Tsuruta, T. Imamoto, K. Yamaguchi, Evaluation of the relative Lewis acidities of lanthanoid(III) compounds by tandem mass spectrometry, Chem. Commun. (1999) 1703–1704, https://doi.org/10.1039/A905569J.

[12] H. Forsberg, V.T. Spaziano, T.M. Balasubramanian, G.K. Liu, S.A. Kinsley, C. A. Duckworth, J.J. Poteruca, P.S. Brown, J.L. Miller, Use of lanthanide(III) ions as catalysts for the reactions of amines with nitriles, J. Organomet. Chem. 52 (1987) 1017–1021, https://doi.org/10.1021/jo00382a009.

[13] N. Nomura, A. Taira, A. Nakase, T. Tomioka, M. Okada, Ring-opening polymerization of lactones by rare-earth metal triflates and by their reusable system in ionic liquids, Tetrahedron 63 (2007) 8478–8484, https://doi.org/10.1016/j.tet.2007.05.073.

[14] F. Hu, S. Xie, L. Jiang, Z. Shen, Living cationic ring-opening polymerization of 2-oxazolines initiated by rare-earth metal triflates, RSC Adv. 4 (2014) 59917–59926, https://doi.org/10.1039/C4RA11404C.

[15] L. You, T.E. Hogen-Esch, Y. Zhu, J. Ling, Z. Shen, Brønsted acid-free controlled polymerization of tetrahydrofuran catalyzed by recyclable rare earth triflates in the presence of epoxides, Polymer 53 (2012) 4112–4118, https://doi.org/10.1016/j.Polymer.2012.07.047.

[16] P. Castell, M. Galià, A. Serra, J.M. Salla, X. Ramis, Study of lanthanide triflates as new curing initiators for DGEBA, Polymer 41 (2000) 8465–8474, https://doi.org/10.1016/S0032-3861(00)00275-5.

[17] C. Mas, A. Serra, A. Mantecón, J.M. Salla, X. Ramis, Study of lanthanide triflates as new curing initiators for cycloaliphatic epoxy resins, Macromol. Chem. Phys. 202 (2001) 2554–2564, https://doi.org/10.1002/1521-3935(20010801)202:12<2554::AID-MACP2554>3.0.CO;2-C.

[18] M. Arasa, X. Ramis, J.M. Salla, A. Mantecón, A. Serra, A study of the degradation of ester-modified epoxy resins obtained by cationic copolymerization of DGEBA with γ-lactones initiated by rare earth triflates, Polym. Degrad. Stab. 92 (2007) 2214–2222, https://doi.org/10.1016/j.polymdegradstab. 2007.01.037.

[19] S. Gonzalez, X. Fernandez-Francos, J. Maria Salla, A. Serra, A. Mantecón, X. Ramis, New thermosets obtained by cationic copolymerization of DGEBA with γ-caprolactone with improvement in the shrinkage. II. Time–temperature–transformation (TTT) cure diagram, J. Appl. Polym. Sci. *104* (**2007**) 3406–3416, https://doi.org/10.1002/app.26021.

[20] S. Kobayashi, M. Sugiura, H. Kitagawa, W.W.-L. Lam, Rare-earth metal triflates in organic synthesis, Chem. Rev. 102 (2002) 2227–2302, https://doi.org/10.1021/cr010289i.

[21] M. Matsumoto, R.R. Dasari, W. Ji, C.H. Feriante, T.C. Parker, S.R. Marder, W. R. Dichtel, Rapid, low temperature formation of imine-linked covalent organic frameworks catalyzed by metal triflates, J. Am. Chem. Soc. 139 (14) (2017) 4999–5002, https://doi.org/10.1021/jacs.7b01240.

[22] S. Gulyuz, B. Kiskan, Combination of polyethylenimine and vanillin-based benzoxazine as a straightforward self-healable system with excellent film-forming ability, Macromolecules 57 (5) (2024) 2078–2089, https://doi.org/10.1021/acs.macromol.4c00005.

[23] N. Giuseppone, J-L. Schmitt, E. Schwartz, J-M. Lehn, Scandium (III) catalysis of transimination reactions. Independent and constitutionally coupled reversible processes, J. Am. Chem. Soc. 2005, 127, 5528–5539, Doi: https://doi.org/10.1021/ja042469q.

[24] N. Giuseppone, J.-L. Schmitt, J.-M. Lehn, Generation of dynamic constitutional diversity and driven evolution in helical molecular strands under Lewis acid catalyzed component exchange, Angew. Chem. Int. Ed. 43 (2004) 4902–4906, https://doi.org/10.1002/anie.200460343.

[25] F. Guerrero, F. Gamardella, X. Ramis, S. De la Flor, A. Serra, The use of lanthanide triflates in the preparation of poly(thiourethane) covalent adaptable networks, Polymer 283 (2023) 126262, https://doi.org/10.1016/j.polymer.2023.126262.

[26] A. Roig, J. Padilla, S. De la Flor, A. Serra, Bio-based poly(amido-imide) CANs catalysed by lanthanide triflates: high creep resistance and superior reprocessability, Eur. Polym. J. 224 (2025) 113700.

[27] S.K. Schoustra, M.M.J. Smulders, Metal coordination in polyimine covalent adaptable networks for tunable material properties and enhanced creep resistance, Macromol. Rapid Commun. 44 (2023) 2200790, https://doi.org/10.1002/marc.202200790.

[28] M. Chini, P. Crotti, L. Favero, F. Macchia, M. Pineschi, Lanthanide (III) trifluoromethanesulfonates as extraordinarily effective new catalysts for the aminolysis of 1,2-epoxides, Tetrahedron Lett. 35 (1994) 433–436, https://doi.org/10.1016/0040-4039(94)85073-9.

[29] D.H. Johnston, D.F. Shiver, Vibrational study of the Trifluoromethanesulfonate anion: unambiguous assignment of the asymmetric stretching modes, Inorg. Chem. 32 (1993) 1045–1047, https://doi.org/10.1021/ic00058a050.

[30] L. González, X. Ramis, J.M. Salla, A. Mantecón, A. Serra, The degradation of new thermally degradable thermosets obtained by cationic curing of mixtures of DGEBA and 6,6-dimethyl (4,8-dioxaspiro[2.5]octane-5,7-dione), Polym. Degrad. Stab. *92* (**2007**) 596–604, https://doi.org/10.1016/j.polymdegradstab.

[31] N.N. Greenwood, A. Earnshaw, Chemistry of the Elements, 2nd ed., U.K., University of Leeds, School of Chemistry, 1997.

[32] J. Zheng, Z.M. Png, S.H. Ng, G.X. Tham, E. Ye, S.S. Goh, X.J. Loh, Z. Li, Vitrimers: current research trends and their emerging applications, Mater. Today 51 (2021) 568–625, https://doi.org/10.1016/j.mattod.2021.07.003.

[33] L. Li, X. Chen, K. Jin, J.M. Torkelson, Vitrimers designed both to strongly suppress creep and to recover original cross-link density after reprocessing: quantitative theory and experiments, Macromolecules 51 (2018) 5537–5546, https://doi.org/10.1021/acs.macromol.8b00922.

[34] H. Tsuruta, K. Yamaguchi, T. Imamoto, Evaluation of the relative Lewis acidities of lanthanoid (III) compounds by tandem mass spectrometry, Chem. Commun. (1999) 1703–1704, https://doi.org/10.1039/A905569J.